We are IntechOpen,
the world's leading publisher of
Open Access books
Built by scientists, for scientists

4,800
Open access books available

122,000
International authors and editors

135M
Downloads

Our authors are among the

154
Countries delivered to

TOP 1%
most cited scientists

12.2%
Contributors from top 500 universities

CLARIVATE ANALYTICS
BOOK CITATION INDEX
INDEXED

WEB OF SCIENCE™

Selection of our books indexed in the Book Citation Index
in Web of Science™ Core Collection (BKCI)

Interested in publishing with us?
Contact book.department@intechopen.com

Numbers displayed above are based on latest data collected.
For more information visit www.intechopen.com

Synthesis and Characterization of Fe-Imogolite as an Oxidation Catalyst

Masashi Ookawa

Additional information is available at the end of the chapter

1. Introduction

Imogolite is a hydrated aluminosilicate with a unique tubular structure, which is found in volcanic ash soil and is shown in Figure 1. It was first discovered in glassy volcanic ash soil in Japan and was named after the soil in Hitoyoshi, Kumamoto Prefecture [1]. Its chemical composition is $(OH)_3Al_2O_3Si(OH)$.

Figure 1. Photograph of natural imogolite films in soil.

The tubular structure of imogolite was proposed by Cradwick et al. [2] based on results from electron diffraction observation and is shown in figure 2. The tube wall consists of a

single continuous $Al(OH)_3$ (gibbsite) sheet and orthosilicate anions (O_3SiOH groups) associated with each vacant octahedral site of the gibbsite sheet. The imogolite has an outer diameter of ca. 2 nm and an inner diameter of ca. 1 nm.
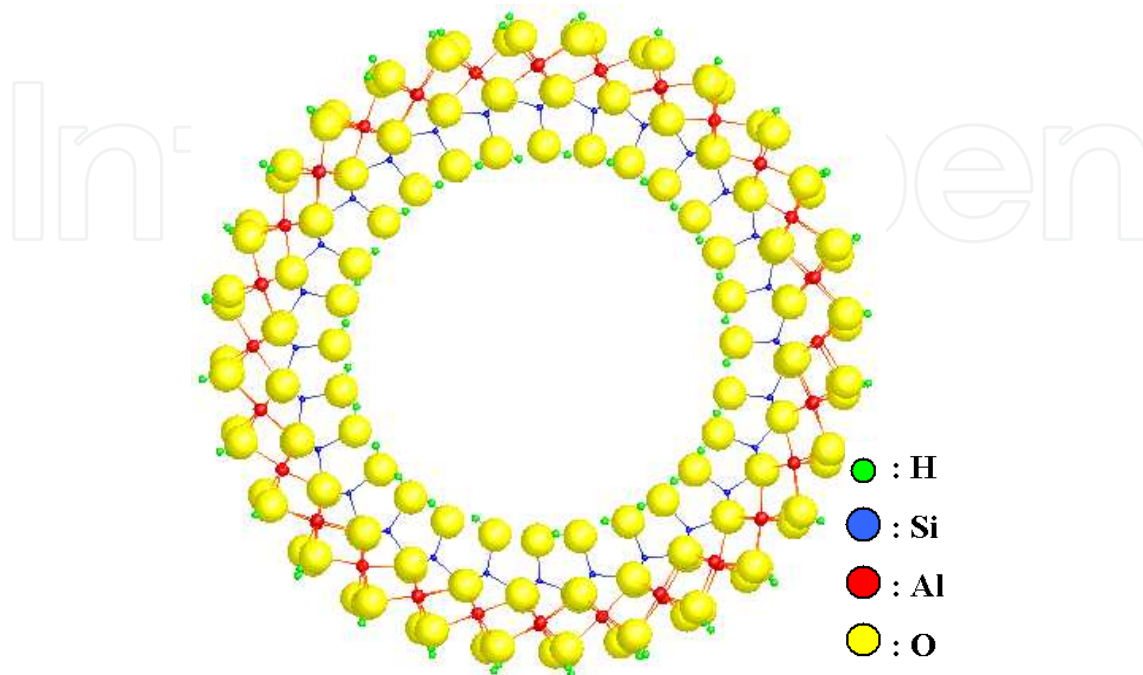

Figure 2. A cross-section of the structural model of an imogolite tube.

Recently, imogolite has drawn a new attention as a new nano-material because of its unique nano-scale tubular structure similar to that of a single-walled carbon nanotube [3]. Studies on synthesis [4-9], mechanisms of formation [10], structural evolution [11, 12], stability [13, 14], electronic states [14, 15] and application have been carried out. Proposed applications, such as a polymer composite [16,17], a fuel gas storage [18], an absorbent [19], an exchange material for heat pump system [20], a humidity-controlling material [6] and an anti-deweling material [6] have been discussed.

Application as a catalyst or a catalyst support also attracts attention because it is expected to have a shape-selective characteristic property as molecular sieving zeolites due to its unique tubular structure. However, few investigations [21, 22] have been reported using natural imogolite as a catalyst because the extraction of pure imogolite from the soil is difficult and time consuming [21]. Therefore, synthesis of imogolite has become necessary in order to utilize it as a functional material.

We synthesized imogolite containing Fe^{3+} ions (Fe-imogolite) using $NaSiO_4$, $FeCl_3$ and $AlCl_3$ to investigate its catalytic properties [23]. Because of its chemical stability, an incorporation of another element is necessary to generate a chemical function. We found that it served as a catalyst of liquid-phase oxidation reactions of some hydrocarbons.

In this chapter, the synthetic methods, characterization and the general properties of imogolite is described at first. And then the characterization and catalytic properties of Fe-imogolite obtained from our researches is described.

2. Synthetic imogolite

In the latter half of the 1970's, synthesis of imogolite was succeeded from a dilute solution. Recently, various synthesis methods have been investigated and many characterizations have been carried out. In this section, synthesis methods, structural characterization and catalytic properties of synthetic imogolite are described.

2.1. Synthesis method of imogolite

Farmer et al. reported [24] the synthesis method of imogolite in 1977. Imogolite was synthesized from a dilute solution containing of hydroxyaluminum cations (2.4 mmol L^{-1}) and orthosilicic acid (1.4 mmol L^{-1}). Afterward, the solution was adjusted to pH 5 with sodium hydroxide, 1 mmol L^{-1} of hydrochloric acid solution and 2 mmol L^{-1} of acetic acid. Imogolite was obtained in this solution by heating it near the boiling point. Wada et al. [25] later also investigated the effects of Al-to-OH^{-} (as sodium hydroxide) ratio to synthesizing imogolite and allophane using a dilute inorganic solution.

A diluted inorganic solution is necessary to form imogolite in these methods, because preventing the condensation of orthosilicic acid and the formation inhibition of it by anions is important to form the nanotube structure. However, it is difficult to obtain a large sample. Suzuki et al. [6] developed a synthetic method of producing imogolite using a concentrated inorganic solution. Sodium orthosilicate was used as a starting material to prevent the condensation of orthosilicic acid. Furthermore, a desalination process is carried out by centrifugation. We have synthesized Fe containing imogolite based on improving Suzuki's method which will be described below in detail.

More recently, new synthesis methods of imogolite have been reported. Levard et al. [8] synthesized it from a decimolar concentration solution at 95 °C for 60 days. Abidin et al. [9] proposed a new supplying method of a silicon source using colloidal silica for the synthesis of imogolite.

2.2. Characterization of imogolite

2.2.1. Morphology

Transmission electron microscopy (TEM) or scanning electron microscopy (SEM) is used mostly in order to observe the morphology and structure of imogolite nanotubes. Figure 3 shows an SEM image of synthetic imogolite.

Bursill et al. [2] have observed the various aggregations of them such as randomly oriented single tube, close-packed arrays or fiber bundles by high resolution TEM.

On the other hand, atomic force microscopy (AFM) is a powerful tool to investigate them under ambient conditions. The tapping-mode AFM especially shows the morphological features of the synthetic imogolite clearly [26, 27]. Figure 4 shows the tapping mode AFM image of synthetic imogolite. Fibrous materials with a length of 100 - 1000 nm can be observed in this image.
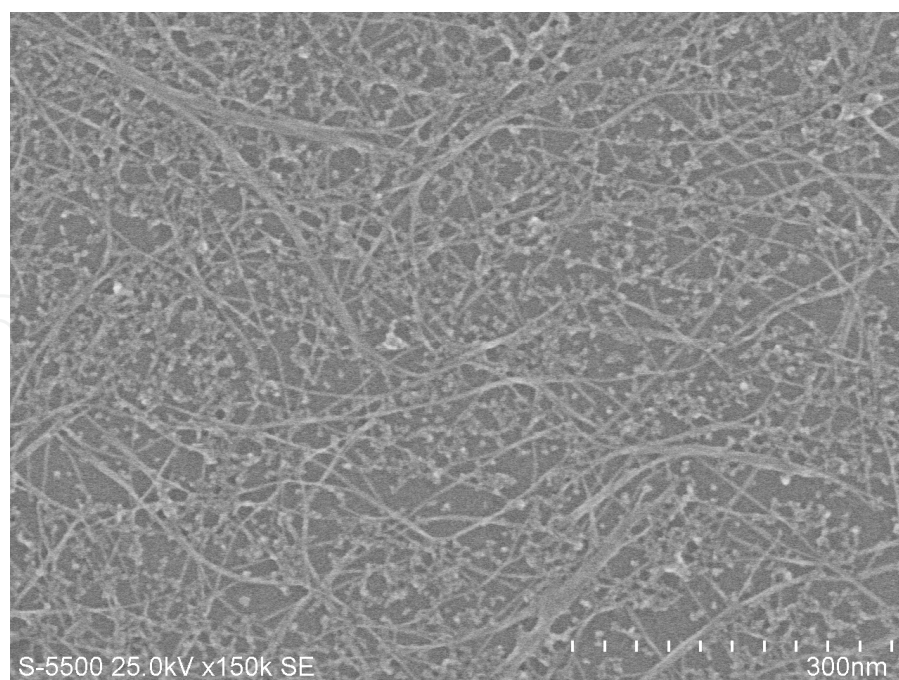
Figure 3. The FE-SEM image of synthetic imogolite.

2.2.2. Structural characterization

The analytical methods, such as X-ray diffraction (XRD), infrared (IR) spectroscopy and solid state nuclear magnetic resonance (NMR) are used in order to identify or characterize imogolite. In this section, the features of imogolite obtained using these analytical methods are mentioned.

The XRD profiles which were obtained by Cu Kα irradiation are given in Figure 5. Imogolite is characterized by three broad peaks in the low angle region. There are three peaks at 2θ = 5.1°, 11° and 15.6° in the XRD profile of natural imogolite and at 2θ = 4.6°, 9.6° and 14.3° in that of synthetic imogolite. The difference in peak position is due to the difference in the diameter of a tube of a natural and synthetic imogolite [7, 24]. The diameter of 1.8 - 2.2 nm in natural imogolite [1] and 2.7 - 3.2 nm in synthetic imogolite [25] were reported.

FT-IR spectra of Natural and synthetic imogolite, which are shown in figure 6, have a characteristic absorption that appears as a doublet at around 1000 cm^{-1}. These absorptions are attributed to Si-O (higher frequency) and Si-O-Al (lower frequency) stretching [28]. These samples also have some absorption bands in the region from 400 cm^{-1} to 750 cm^{-1}. The absorption bands at 685 cm^{-1}, 563 cm^{-1} and 427 cm^{-1} in natural imogolite arise from various Al-O vibrations [29].

Imogolite is also characterized by ^{29}Si and ^{27}Al solid state NMR [30-34]. Magic angle spinning (MAS) techniques are used in general in order to obtain a high resolution NMR spectrum of sold state. Goodman et al. [34] have carried out ^{29}Si and ^{27}Al MAS NMR measurements of synthetic imogolite. The peak is observed at -78.8 ppm in ^{29}Si MAS NMR spectrum of it as well as natural imogolite. Barron et al. [30] have shown that the observed
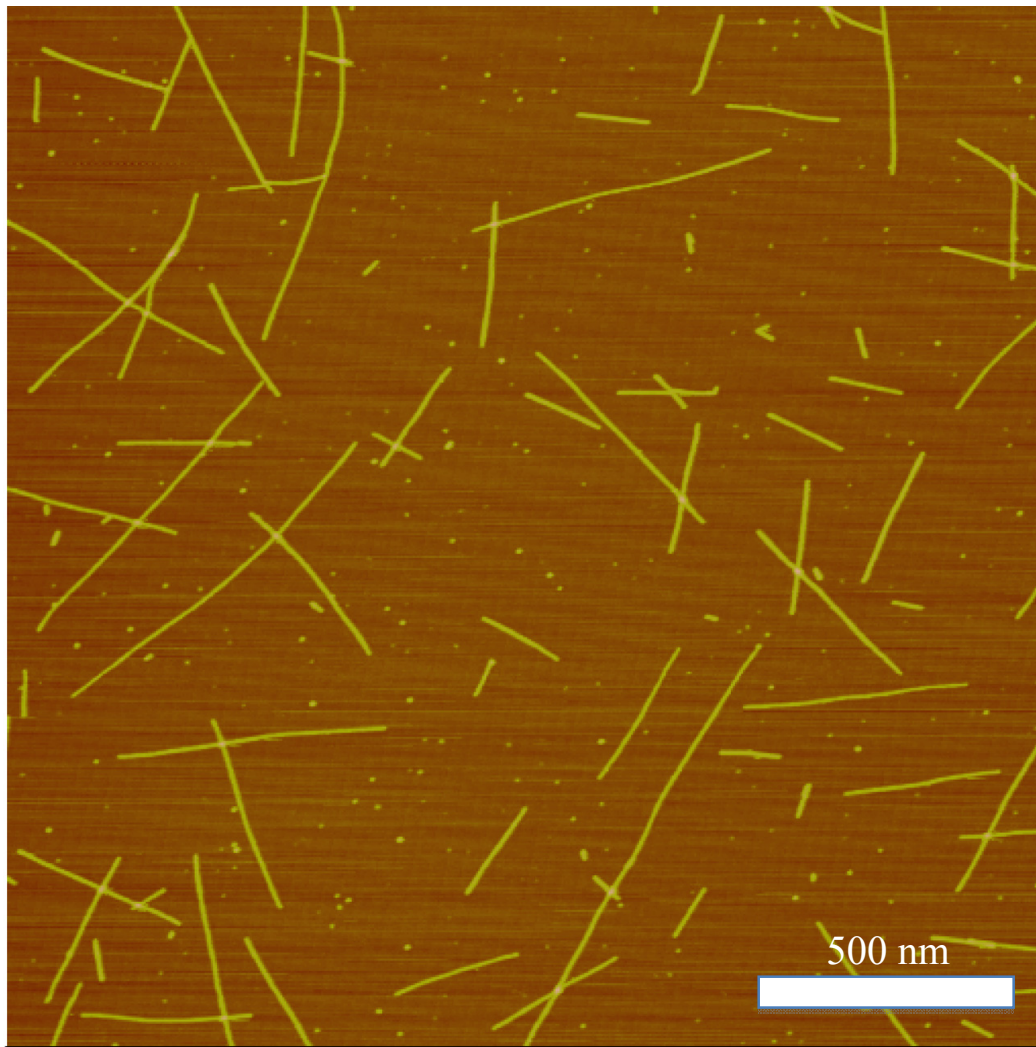
Figure 4. The tapping mode AFM image of synthetic imogolite.
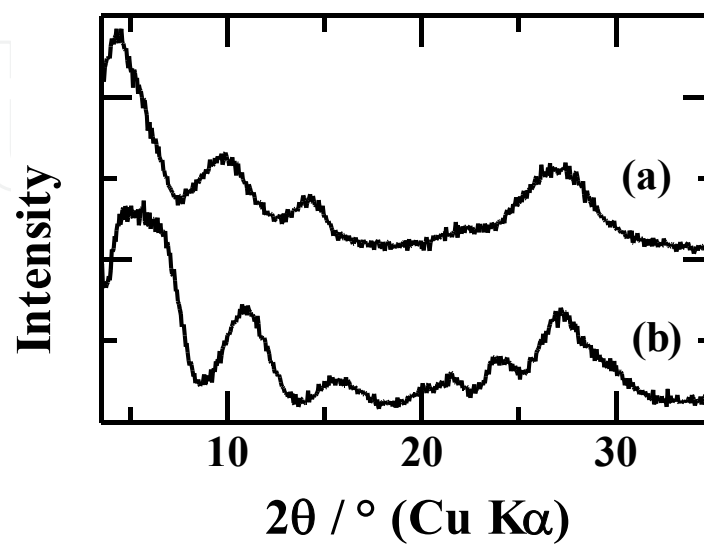

Figure 5. XRD profiles of synthetic imogolite (a) and natural imogolite (b).

chemical shift of natural imogolite is consistent with silicon tetrahedra which are isolated by coordination through oxygen with three aluminum atoms and one proton. On the other hand, ^{27}Al MAS NMR spectrum of imogolite has one peak at 0 ppm and it is attributed to the six coordinated octahedral Al^{3+} species [31-34].
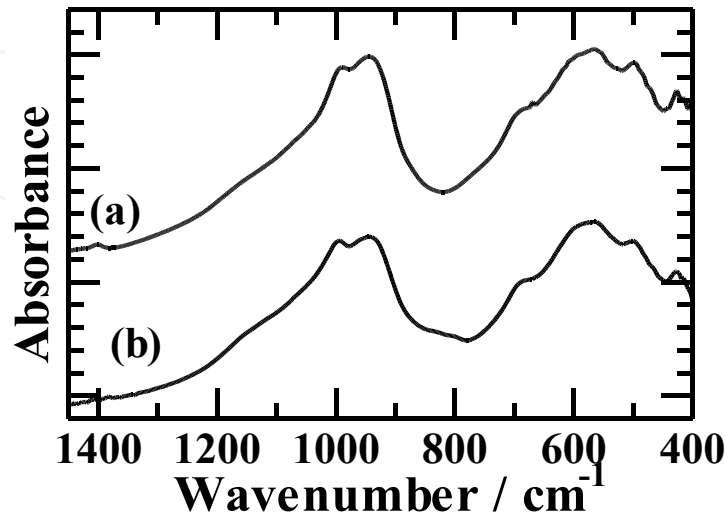

Figure 6. FT-IR spectra of synthetic imogolite (a) and natural imogolite (b).

2.2.3. Thermal transformation of synthetic imogolite

The differential thermal analysis (DTA) and thermo gravimetric analysis (TGA) traces of synthetic imogolite are shown in Figure 7. Two broad endothermic peaks with a weight loss and an exothermic peak without a weight change were observed.
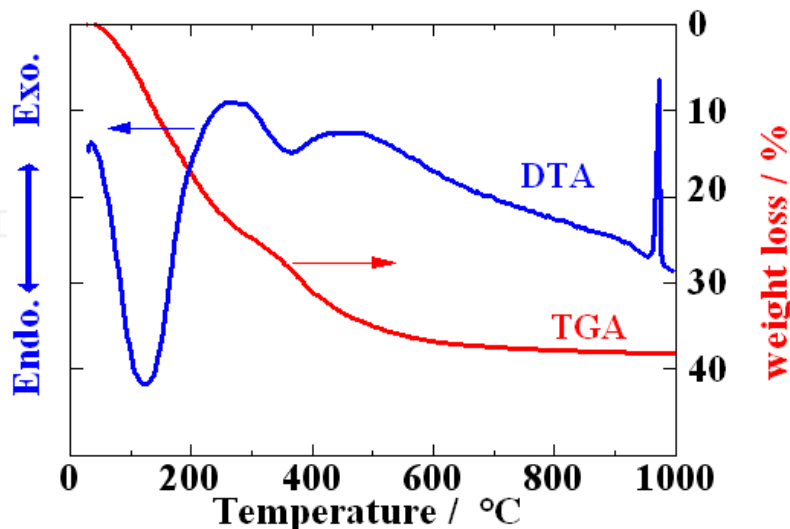

Figure 7. DTA-TGA curves of synthetic imogolite.

MacKenzie et al. [31] investigated thermal transformation of natural imogolite by using DTA-TGA, ^{29}Si MAS NMR and ^{27}Al MAS NMR and proposed the structural models which were changed by heating. The results of DTA-TGA showing thermal transformation of

imogolite are explained based on their literature. The endothermic peaks at 110 °C and 400 °C were attributed to the loss of adsorbed water and dehydroxylation, respectively. Amorphism of imogolite occurred by these dehydroxylations. The exothermic peak at 950 °C was attributed to crystallization to mullite ($Al_6Si_2O_{13}$). Donkai *et al.* [11] investigated thermal transformation of natural imogolite up to 1600 °C using XRD and IR and reported the formation of tridymite (SiO_2) with mullite crystals above 1200 °C. Hatakeyama et al. [34] investigated the transformation heat-treated synthetic imogolite by using ^{27}Al MAS NMR and ^{27}Al multiple-quantum magic-angle-spinning (MQMAS) NMR. These results show five- and four-coordinated Al is formed above 350 °C in amorphous materials clearly.

2.2.4. Catalytic properties

It has been known that imogolite has surface acidity [35]. The acid strength of it is increased by heat treatment. Natural imogolite calcined at various temperatures were used as catalysts for the isomerization of 1-butene [21]. This reaction proceeded effectively over samples calcined at 400 °C. The decomposition reaction of organic peroxides also was investigated using Cu^{2+} loaded imogolite calcined at 500 °C. Furthermore, it was mentioned that imogolite calcined at temperature up to 750 °C exhibited the shape selective adsorption. Bonelli et al. [36] have studied *in situ* IR spectroscopy of synthetic imogolite which adsorbed CO, ammonia, methanol or phenol and catalytic tests using gas-phase phenol reactions with methanol. They showed that a small amount of Al^{3+} Lewis acid sites to adsorb CO existed, the adsorbed ammonia on imogolite evacuated at 150 °C was observed as NH_4^+ species and, in addition, a probe such as CO, ammonia, methanol or phenol could interact with inner silanols. The reaction of phenol with methanol was performed over imogolite after thermal treatment at 300 °C and at 500 °C. The activity was shown over samples heated at 500 °C and o-cresol and anisole were obtained as products.

We have investigated the acidic property of imogolite without heat treatment [37]. At first, we attempted an isomerization reaction of α-pinene on synthetic imogolite. It is known that the isomerization products of α-pinene depend on the acid or base property of the catalyst. In the case of acid catalysts, α-pinene isomerize to limonene, camphene and tricyclene [38]. Prior to the reaction imogolite was dried at 120 °C for 12 hours. The isomerization reaction of α-pinene was carried out at 80 °C for 3 hours or 24 hours using an evacuated batch reactor. In a typical experiment, the reactor was loaded with 12.6 mmol of α-pinene and 50 mg of catalyst. The α-pinene did not react on it. It was reported that imogolite had a weak acid property, however it was not detected in this reaction.

Although isomerization of α-pinene did not occurre, some oxidation products of it were detected slightly. So the oxidation reaction of cyclohexene using hydrogen peroxide was carried out to test the possibility as an oxidation catalyst.

In a typical catalytic experiment for oxidation [38], the reaction was carried out by using 25 mmol of cyclohexene, 25 mmol of H_2O_2 (30 wt%) and 30 ml of acetic acid or acetonitrile as a

solvent with 100 mg of catalyst under being stirred at 50 °C. The results of the oxidation reaction of cyclohexene with H_2O_2 are listed in Table 1. Without a catalyst the oxidation products such as trans-1,2-cyclohexanediol, cis-1,2-cyclohexanediol and 2-cyclohexene-1-ol were observed using acetic acid as solvent. With imogolite the yield of these oxidation products was increased, but the selectivity was almost the same as the control experiment. This result indicates that imogolite has the potential of concentration and acts as a field of reaction to increase collision frequency.

Product		1-ol	trans-diol	cis-diol
Yield	imogolite	32.3	21.5	2.9
/ %	no catalyst	14.6	12.0	1.3
Selectivity	imogolite	56.9	38.0	5.1
/ %	no catalyst	52.3	43.2	4.5

Table 1. Oxidation of cyclohexene with H_2O_2 over imogolite in acetic acid as a solvent. [38] Reaction condition: temperature 50 °C, time 6h, imogolite 100 mg
 1-ol : 2-cyclohexene-1-ol, trans-diol : trans-1,2-cyclohexanediol, cis-diol: 1,2-cyclohexanediol

In the case of using acetonitrile as the solvent, the oxidation products were not detected for 27 hours of reaction time. In the case of imogolite, 2-cyclohexene-1-ol and 1,2-epoxycyclohexene were produced with 0.5 % and 0.8 % yields, respectively. This results shows that imogolite has the possibility as an oxidation catalyst.
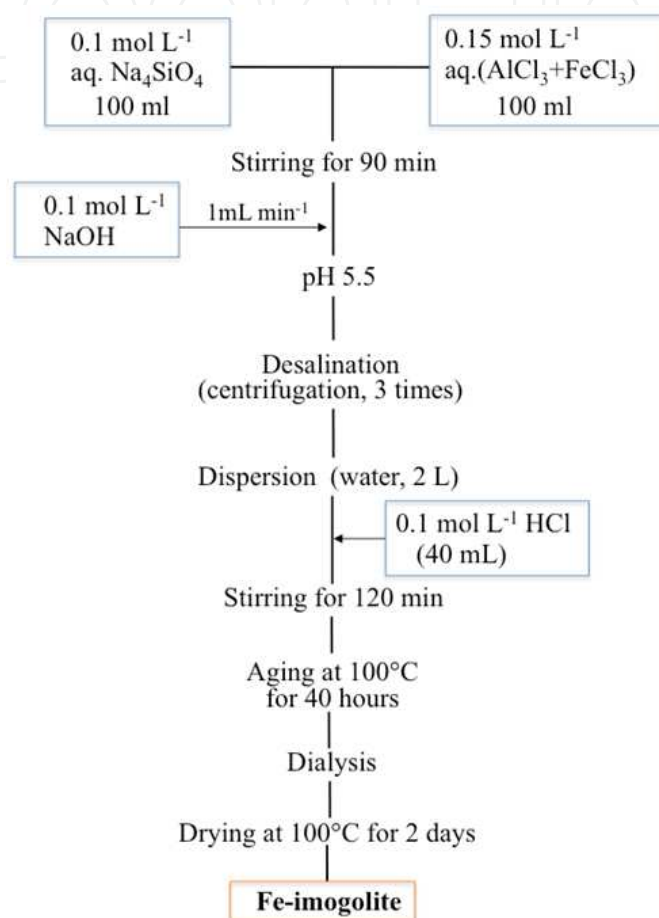
3. Fe-imogolite

Although we found the new possibility of synthetic imogolite as an oxidation catalyst, a chemical modification of imogolite like an introduction of Fe^{3+} ion was necessary to promote the reaction because imogolite is chemically stable. In this section, our results of the synthetic method, characterization and catalytic test of Fe-imogolite are described.

3.1. Synthesis of Fe-imogolite

Fe-imogolite was synthesized based on improving Suzuki's method [6, 7]. The typical method [23] is described here and its flowchart is shown in Scheme 1.

1. We prepared 100 mL of 0.15 mol L^{-1} aqueous solutions consist of $FeCl_3$ and $AlCl_3$ with x = 0.05 (x = Fe/Al+Fe, atomic ratio). Another way of saying, 0.00075 mol $FeCl_3 \cdot 6H_2O$ and 0.01425 mol $AlCl_3 \cdot 6H_2O$ were dissolved in 100 mL of water.
2. 100 mL of 0.1 mol L^{-1} Na_4SiO_4 aqueous solution was prepared.
3. Na_4SiO_4 aqueous solution was added to $AlCl_3$ and $FeCl_3$ mixture and the solution was stirred for 90 minutes.
4. 0.1 mol L^{-1} NaOH aqueous solution was added to the solution consist of Na_4SiO_4, $FeCl_3$ and $AlCl_3$ at the rate of 1.0 mL min^{-1} under stirring until the pH of the mixture become 5.5.

5. The salt-free precursor was obtained from thick solution by centrifugal separation three times.
6. It was dispersed in 2 L of water and 40 mL of 0.1 mol L^{-1} HCl was added.
7. The solution was stirred for two hours at room temperature.
8. It was aged at 100 °C for 40 hours.
9. This aging solution was dialyzed and then dried at 100 °C for two days.
10. The film-like Fe-imogolite was obtained.

0.1 mol L^{-1}
aq. Na$_4$SiO$_4$
100 ml

0.15 mol L^{-1}
aq.(AlCl$_3$+FeCl$_3$)
100 ml

Stirring for 90 min

0.1 mol L^{-1}
NaOH

1mL min^{-1}

pH 5.5

Desalination
(centrifugation, 3 times)

Dispersion (water, 2 L)

0.1 mol L^{-1} HCl
(40 mL)

Stirring for 120 min

Aging at 100°C
for 40 hours

Dialysis

Drying at 100°C for 2 days

Fe-imogolite

Scheme 1. Flowchart of a synthetic method of Fe-imogolite.

3.2. Characterization of Fe-imogolite

Fe containing samples with x = 0, 0.05, 0.1 were prepared in order to survey the effect of Fe^{3+} contents in starting solutions to formation of imogolite nanotubes,. The XRD profiles and IR spectra of these samples are shown in Figure 8.

As mentioned above, imogolite (x = 0) was characterized by three broad peaks in the low angle region of the XRD profile and a doublet at around 1000 cm^{-1} in the FT-IR spectrum. In the case of x = 0.1, it lacks the three broad peaks in XRD and a doublet in FT-IR, meaning the sample does not have the imogolite structure. In the case of x=0.05, the XRD profile and FT-IR spectrum were similar to the imogolite. The intensity of the three broad peaks is weaker

than that of imogolite because XRD measurements were carried out using Cu Kα irradiation. The color and the profiles of XRD and FT-IR indicate the sample with x=0.05 is considered Fe containing imogolite and is thus called Fe-imogolite.
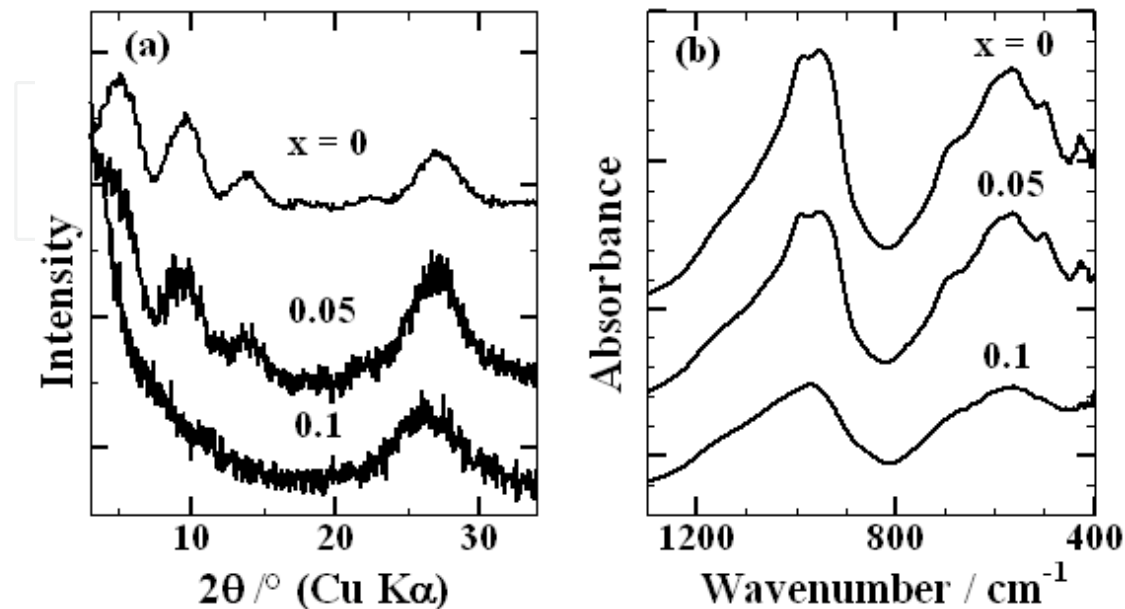

Figure 8. Characterization of Fe containing samples with x (= Fe/Al+Fe, atomic ratio) =0, 0.05, 0.1. XRD profiles (a) and FT-IR spectra (b) [23].

In order to investigate the state of iron ions in Fe-imogolite, it was compared with the Fe^{3+} ion adsorbed on imogolite The adsorbed Fe^{3+} ions sample was prepared by adsorbing $FeCl_3$ onto imogolite from aqueous solution of $FeCl_3$ and is called $FeCl_3$/imogolite. These samples are both reddish brown and the absorption bands of them were observed at the region above 15,000 cm^{-1} in diffuse reflectance ultraviolet visible (UV-VIS) spectra (Figure 9). The absorption bands of Fe^{3+} in many minerals are observed in this region.

It has been known that when the tetrahedral species of Fe^{3+} exist, the pre-edge peak appears strongly in X-ray absorption near edge structure (XANES) spectra. XANES spectra of Fe K-edge (7.111 keV) are shown in Figure 10. The pre-edge peak was not observed in the spectrum of Fe-imogolite nor $FeCl_3$/imogolite or Fe_2O_3. Thus it is clear that the state of iron in Fe-imogolite is octahedral Fe^{3+} ion from the results of UV-VIS and XANES spectra.

Figure 11 shows their Fourier transforms (FT) spectra of Fe-imogolite, $FeCl_3$/imogolite and Fe_2O_3. FT spectrum as radial structure function was obtained by Fourier transformation of k^3-weighted extended X-ray absorption fine structure (EXAFS) function. The FT spectrum of Fe-imogolite is different to that of $FeCl_3$/imogolite or Fe_2O_3. It can be concluded that the state of Fe^{3+} in Fe-imogolite is different to the state of Fe^{3+} ions adsorbed on imogolite. We speculate that Fe^{3+} replaced the Al^{3+} sites in imogolite from these results.

The tapping mode AFM image of Fe-imogolite is shown in figure 12 [39]. The fibrous morphology was observed similar to the synthetic imogolite. It was found that the tube diameter was almost uniform and estimated to be 2.2-2.4 nm from section analysis.
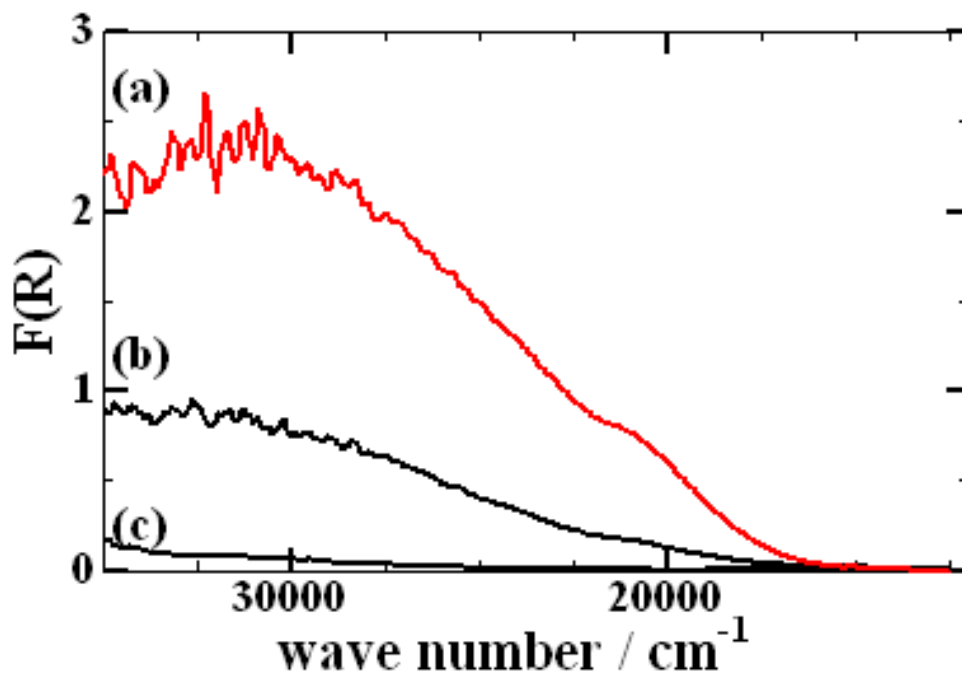
Figure 9. Diffuse reflectance UV-VIS spectra of (a) Fe-imogolite, (b) FeCl$_3$/imogolite and (c) imogolite [23].
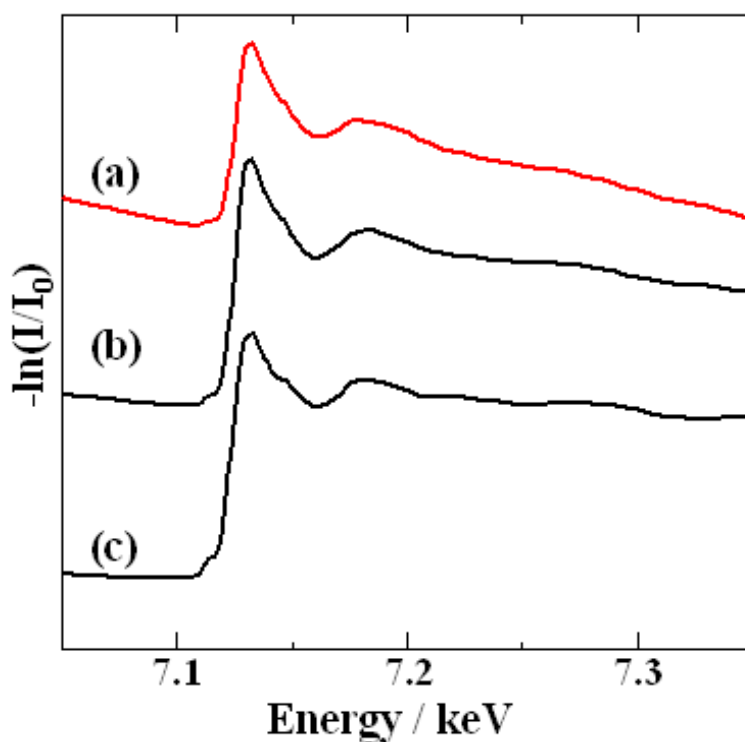

Figure 10. Fe K-edge XANES spectra of (a) Fe-imogolite, (b) FeCl$_3$/imogolite and (c) Fe$_2$O$_3$ (hematite) [23].
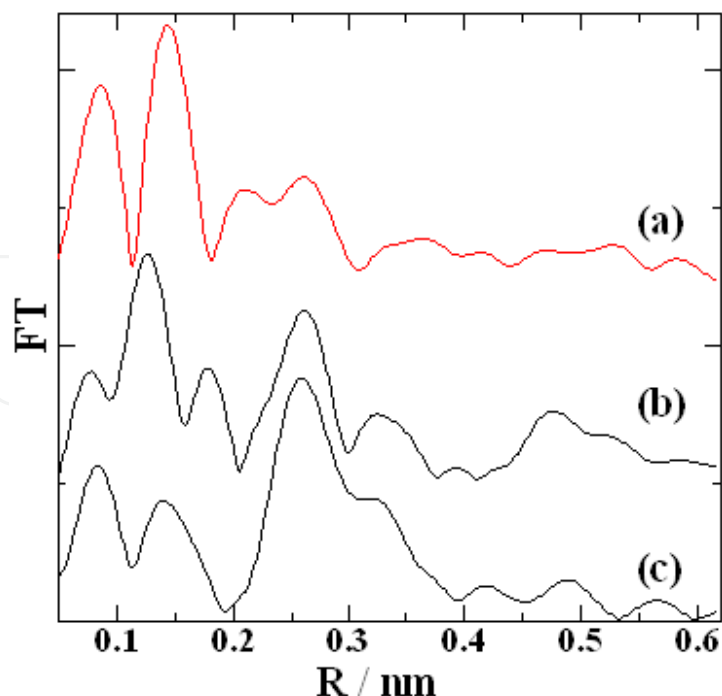
Figure 11. FT spectra of Fe K-edge k^3-weighted EXAFS functions. (a) Fe-imogolite, (b) FeCl$_3$/imogolite and (c) Fe$_2$O$_3$ (hematite) [23].
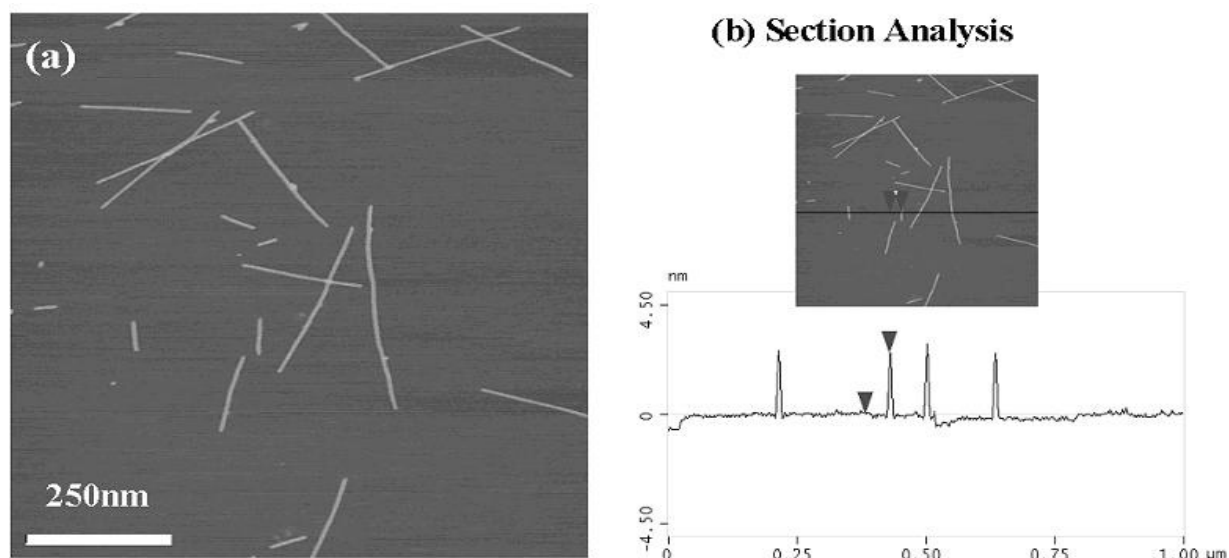

Figure 12. AFM image of Fe-imogolite (a) and section analysis (b). The height profile (right bottom) shows the height on black line in AFM picture (right top) [39].

3.3. Oxidation of hydrocarbons using Fe-imogolite catalyst

3.3.1. Oxidation of cyclohexene [23]

The oxidation of cyclohexene was carried out using cyclohexene, H$_2$O$_2$ and acetonitrile as a solvent with catalysts under being stirred at 50 °C for 24 hours. No product was detected without a catalyst. In the case of imogolite, 2-cyclohexene-1-ol and 1,2-epoxycyclohexane (EP)

were produced slightly as stated above. EP was also detected in separate experiments using gibbsite, boehmite and Al_2O_3 as catalysts. Mandelli et al. [40] have reported the epoxidation of cyclohexene using H_2O_2 over Al_2O_3. It was attributed that these oxidation compounds may be produced on the outer surface of the imogolite. The oxidation reaction was promoted by Fe-imogolite and not only alcohol and epoxy compounds but trans-1,2-cyclohexanediol, cis-1,2-cyclohexanediol and 2-cyclohexene-1-one were also obtained as products.

3.3.2. Oxidation of aromatic hydrocarbon [23, 39]

Phenol is one of the most important chemicals in the fields of fiber and medicine manufacturing. More than 90% of phenol is produced by the cumen process, which is a three-step process and produces acetone as a by-product. The development of a one-step process for phenol synthesis by the direct oxidation of benzene is important when concerned with green chemistry as an environment-friendly technique. It was found that benzene or other aromatic hydrocarbons were oxidized by H_2O_2 over Fe-imogolite. These results are described.

The reaction of benzene was carried out using 2 mmol of benzene, 11 mmol of H_2O_2 and 10 mL of acetonitrile as a solvent with 100 mg of catalyst under being stirred at 60 °C. The products were analyzed by GC-MASS. The conversion of H_2O_2 was determined by a volumetric analysis with $KMnO_4$.

Figure 13 shows the results of oxidation reactions of benzene using H_2O_2 and compounds containing Fe. None of the oxidation products were detected without catalysts and with $FeCl_3$/imogolite, Fe_2O_3 (hematite) and α-FeOOH (goethite) as a catalyst. It is an interesting finding that only phenol was obtained as an oxidation product by GC-Mass using Fe-imogolite [23].

The oxidation reactions of benzene using four solvents were examined. The results are summarized in Table 2. None of oxidation products were detected in the case of acetic acid and propionic acid as a solvent. It was found that acetonitrile was the most effective for this reaction among the examined solvents. Although the solution turned palish yellow using acetonitrile as a solvent, after the reaction the absorption due to the Fe^{3+} ion was not detected in UV-VIS absorption spectrum. It was suggested that the origin of the coloring could be phenolic tars that could not detected by GC-Mass. A conversion of H_2O_2 was high with all solvent and H_2O_2 efficiency was 2 % using acetonitrile as a solvent. Thus, the decomposition of H_2O_2 was only caused by using other solvents except for acetonitrile.

The results of the oxidation reaction of aromatic hydrocarbons using Fe-imogolite as a catalyst are summarized in Table 3 [39]. Hydroquinone and catechol were produced as products from phenol by the oxidation with H_2O_2. o-Chlorophenol and p-chlorophenol were produced from chlorobenzene. When the side chain is OH group or Cl group, only the benzene ring was oxidized and the ortho and para isomers were obtained. Benzaldehyde, o-cresol and p-cresol were produced from toluene. In the case of benzaldehyde, most of the oxidation product was benzoic acid.

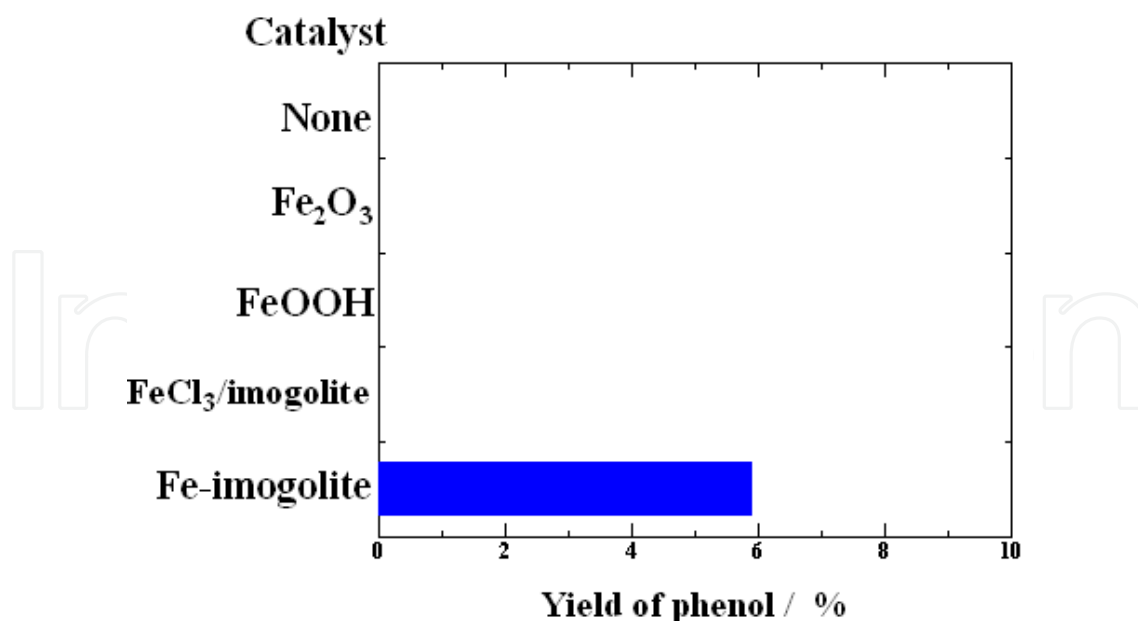**Figure 13.** Results of the oxidation reactions of benzene using Fe-imogolite, FeCl₃/imogolite, Fe₂O₃ (hematite) or FeOOH (geothite) as a catalyst [23].

Solvent	Conversion / %		Yield of Phenol / %
	benzene	H₂O₂	
Acetonitrile	10.6	93	10.6
2-Propanol	tr.	99	tr.
Acetic acid	0.0	95	0.0
Propionic acid	0.0	95	0.0

Table 2. The effects of solvents on the oxidation of benzene [39].
Catalyst Fe-imogolite, temperature = 60 °C, time = 6 h, benzene = 2 mmol,
H₂O₂ = 11.5 mmol, solvent = 10 mL

When the side chain is a hydrocarbon group such as methyl, both the benzene ring and the side chain group were oxidized. It was found that the side chain group was more easily oxidized.

Monfared and Amouei [41] have reported direct oxidation reactions of benzene or some aromatic hydrocarbon compounds over Fe^{3+} loaded Al_2O_3 (Fe^{3+}-Al_2O_3) with H_2O_2 in acetonitrile. In their system, however, *o*-cresol and *m*-cresol as main products were produced from toluene and no oxidation compounds were produced from phenol. It has been shown that the oxidation property of a Fe-imogolite catalyst is different from that of a Fe^{3+} - Al_2O_3 catalyst.

3.3.3. Oxidation of cyclohexane [42, 43]

Oxidation of cycloxane under mild conditions have been very interesting and have attempted widely [44]. Since the oxidation takes place not only on aromatic rings but on

methyl groups by H_2O_2 in acetonitrile over Fe-imogolite catalysts, other organic compounds such as saturated hydrocarbons could be oxidized under this reaction condition. We examined the oxidation of cyclohexane using this catalyst.
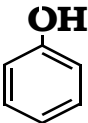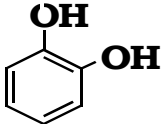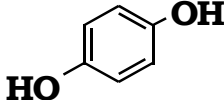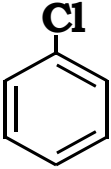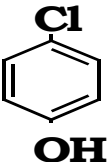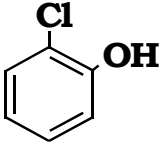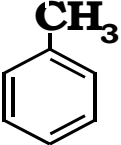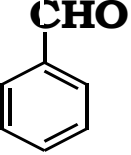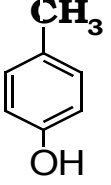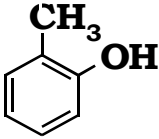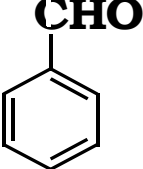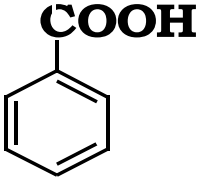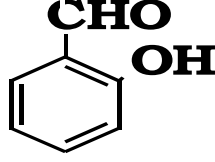
Reactant	Products (Yield* / %)		
phenol	catechol (13.7)	hydroquinone (15.9)	
chlorobenzene	p- chlorophenol (9.7)	o- chlorophenol (4.8)	
toluene	benzaldehyde (5.8)	p- cresol (2.2)	o- cresol (1.3)
benzaldehyde	benzoic acid (71.7)	2-hydroxy-benzaldehyde (1.7)	

Table 3. Oxidation reactions of aromatic hydrocarbons with H_2O_2 over Fe-imogolite [39].
*The yield of product is estimated using the ratio of peak area of GC-Mass.
Temperature = 60°C, time = 6 h, reactant = 2 mmol, H_2O_2 = 11.5 mmol, solvent = 10 mL

The reaction of cyclohexane was carried out using 2 mmol of cyclohexane, 10 mmol of H_2O_2 and 10 ml of acetonitrile as a solvent with 50 mg of catalyst under being stirred at 60 °C for 3 hours. The products were analyzed by GC-Mass and GC with FID detector. The oxidation products were hardly detected without catalysts. With Fe-containing imogolite as a catalyst, this reaction was promoted and three oxidation products were created. Two compounds were easily identified by retention time of standard reagents such as cyclohexanone and cyclohexanol among these products. Another is speculated as cyclohexyl hydroperoxide from fragmentation patterns in the mass spectrum. It was reported [45] that cyclohexyl hydroperoxide was prepared efficiently and selectively using cyclohexane and H_2O_2 over Fe^{3+} ion-changed montmorillonite. We identified one of the oxidation products as cyclohexyl hydroperoxide by the compound obtained following this examination. The conversion of cyclohexane was ca. 25%.

The cyclohexyl hydroperoxide was produced immediately as soon as the reaction started. Additionally, it was detected only in oxidation reactions with Fe_2O_3 or α-FeOOH as a catalyst. It was found that cyclohexanone and cyclohexanol were produced via cyclohexyl hydroperoxide as an intermediate which was obtained by reacting cyclohexane and H_2O_2 (Figure 14).
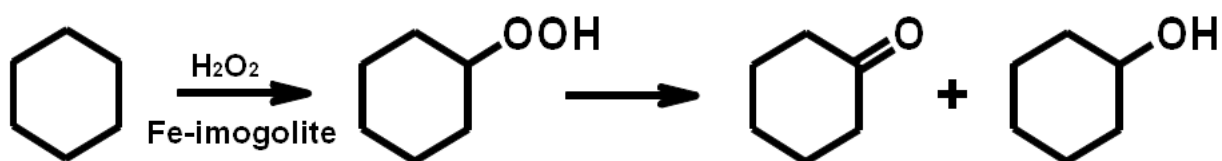

Figure 14. Oxidation reactions of cyclohexane using H_2O_2 over Fe-imogolite [42].

4. Conclusion

Fe-imogolite was synthesized using Na_4SiO_4, $AlCl_3$ and $FeCl_3$ with the atomic ratio Fe / (Al+Fe) = 0.05 and applied as a liquid-phase oxidation catalyst with hydrogen peroxide.

The XRD profile and FT-IR spectrum of this material were similar to the synthetic imogolite. AFM images showed fibrous morphology with ca. 2 nm of diameter. UV-VIS and X-ray absorption spectra revealed the state of Fe^{3+} to be in the octahedral coordination. It was found that Fe-imogolite played as an oxidation catalyst of some hydrocarbons such as cyclohexane, benzene, phenol, toluene and cyclohexane with hydrogen peroxide. The oxidation reaction of cyclohexene was promoted by using Fe-imogolite instead of imogolite as a catalyst. It gave 2-cyclohexene-1-ol, 1,2-epoxycyclohexane, 1,2-cyclohexanediol and 2-cyclohexene-1-one as products. Phenol was produced by the oxidation reaction of benzene. The benzene ring in the aromatic hydrocarbons such as phenol, chlorobenzene, toluene and benzaldehyde was oxidized. Moreover, when the side-chain is a hydrocarbon group, side-chain group was also oxidized. It could be more easily oxidized than the benzene ring. Cyclohexyl hydroperoxide, Cyclohexanone and cyclohexanol were obtained as oxidation products of cyclohexane. It was clarified found that cyclohexanone and cyclohexanol were

produced via cyclohexyl hydroperoxide. The possibility of Fe-imogolite as an oxidation catalyst is shown. However, its reaction mechanism has not been clarified yet. It is necessary to investigation the catalytic properties and the structure of Fe-imogolite further.

Author details

Masashi Ookawa
Department of Chemistry and Biochemistry, Numazu National College of Technology, Numazu, Japan

5. References

[1] Yoshinaga N., Aomine S. (1962) Imogolite in some Ando soils, Soil Sci. Plant Nutr. 8: 114–121.

[2] Cradwick P. D. G., Farmer V. C., Rucell J. D., Masson C. R., Wada K., Yoshinaga N., (1972) Imogolite, a Hydrated Aluminum Silicate of Tubular Structure Nature Phys. Sci. 240:187-189.

[3] Bursill L. A., Peng J. L., Burgeois L. N. (2000) Imogolite: an aluminosilicate nanotube materials, Philos. Mag., 80: 105-117.

[4] Koenderink G.H., Kluijtmans S. G J M, Philipse A. P,(1999) On the Synthesis of Colloidal Imogolite Fibers, J. Colloid. Interface Sci. 216: 429-431.

[5] Hu J., Kannangara G.S. K., Wilson M.A., Reddy N., (2004) The fused silicate rote to protoimogolite and imogolite, J. Non-cryst. Solids, 347:224-230.

[6] Suzuki M., Ohashi F., Inukai K., Maeda M., Tomura S. (2000) Synthesis of Allophane and Imogolite from Inorganic Solution - Influence of Co-Existing lon Concentration and Titration Rate on Forming Precursor -, Nendo Kagaku (J. Clay Sci. Soc. Japan), 40:1-14.

[7] Suzuki M., Inukai K., (2010) Synthesis and Applications of Imogolite Nanotubes, in: Kijima T. editors, Inorganic and Metallic Nanotubular Materials, Topics in Applied Physics, 117: Springer pp. 159-167, DOI: 10.1007/978-3-642-03622-4_12

[8] Levard C., Masion A., Rose J., Doelsch E., Borschneck D., Dominici C., Ziarelli F., Bottero J. –Y., (2009) Synthesis of Imogolite Fibers from Decimolar Concentration at Low Temperature and Ambient Pressure: A Promising Route for Inexpensive Nanotubes, J. Am. Chem. Soc. 131:17080–17081.

[9] Abidin Z., Matsue N., Henmi T. (2008) A New Method for Nano Tube Imogolite Synthesis, Jpn. J. Appl. Phys. 47:5079-5082.

[10] Mukherjee S., Bartlow V. M., Nair S. (2005) Phenomenology of the Growth of Single-Walled Aluminosilicate and Aluminogermanate Nanotubes of Precise Dimensions, Chem. Mater., 17, 4900-4909.

[11] Donkai N., Miyamoto T., Kokubo T., Tanei H. (1992) Preparation of transparent mullite-silica film by heat-treatment of imogolite, J. Mater. Sci., 27: 6193-6196.

[12] MacKenzie K. J. D., Bowden M. E., Brown I. W. M., Meinhold R. H., (1989) Structure and thermal transformations of imogolite studied by ^{29}Si and ^{27}Al high-resolution solid-state nuclear magnetic resonance, Clays Clay Miner. 37: 317-324.

[13] Tamura, K. And Kawamura K. (2002) Molecular Dynamics Modeling of Tubular Aluminum Silicate: Imogolite, J. Phys. Chem. B, 106: 271-278.

[14] Luciana Guimarães L., Andrey N. Enyashin A. N., Frenzel J., Heine T., Duarte H. A., Seifert G. (2007) Imogolite Nanotubes: Stability, Electronic, and Mechanical Properties, ACS Nano, 1:362-368.

[15] Fernando Alvarez-Ramírez, (2007) Ab initio simulation of the structural and electronic properties of aluminosilicate and aluminogermanate natotubes with imogolite-like structure, Phys. Rev. B 76:125421-125434.

[16] Yamamoto K., Otsuka H., Wada S.-I., Sohn D., Takahara A., (2005) Preparation and properties of [poly(methyl methacrylate)/imogolite] hybrid via surface modification using phosphoric acid ester, Polymer, 46, 12386-12392.

[17] Yah W. O., Yamamoto K., Jiravanichanun N. , Otsuka H., Takahara A. (2010) Imogolite Reinforced Nanocomposites: Multifaceted Green Materials, Materials, 3:1709-1745; doi:10.3390/ma3031709.

[18] Ohashi F., Tomura S., Akaku A., Hayashi S., Wada S. -I., (2004)Characterization of synthetic imogolite nanotubes as gas strage, J. Mater. Sci., 39: 1799-1801.

[19] Ackerman W. C., Smith D. M., Huling J. C., Kim Y. -H., Bailey J. K., Brinker C. J., (1993) Gas/Vapor Adsorption in Imogolite: A Microporous Tubular Aluminosilicate, Langmuir, 9, 1051-1057.

[20] Suzuki M., Ohashi F., Inukai K., Maeda M., Tomura S., Mizota T., (2001) Hydration Enthalpy Measurement and Evaluation as Heat Exchangers of Allophane and Imogolite, J. Ceram. Soc. Japan, 109: 681- 685.

[21] Imamura S., Hayashi Y., Kajiwara K., Hoshino H., Kaito C., (1993) Imogolite: A Possible New Type of Shape-Selective Catalyst, Ind. Eng. Chem. Res., 32: 600-603.

[22] Imamura S., Kokubu K., Yamashita T., Okamoto Y., Kajiwara K., Kanai H., (1996) Shape-Selective Copper Loaded Imogolite Catalyst, J. Catal., 160: 137-139.

[23] Ookawa M., Inoue Y., Watanabe M., Suzuki M., Yamaguchi T. (2006) Synthesis and Characterization of Fe containing Imogolite, Clay Sci., 12, Supplement 2: 280-284.

[24] Farmer V. C., Fraser A. R., Tait J. M. (1977) Synthesis of imogolite: A tubular aluminum silicate polymer, J. Chem. Soc. Chem. Comm., 13: 462-463.

[25] Wada S. -I., Eto A., Wada K. (1979) Synthetic allophane and imogolite, J. Soil Sci., 30: 347-355.

[26] Tani M., Liu C., Huang P. M. (2004) Atomic force microscopy of synthetic imogolite, Geoderma, 118: 209-220.

[27] Ohrai, Y., Gozu, T., Yoshida, S., Takeuchi, O., Iijima, S., Shigekawa, H. (2005) Atomic force microscopy on imogolite, aluminosilicate nanotube, adsorbed on Au(111) surface, Jpn. J. Appl. Phys., 44:5397-5399.

[28] Mccutcheon A., Hu J., Kannangara G. S. K., Wilson M. A., Reddy N., (2005) ^{29}Si labelled nanoaluminosilicate imogolite, J. Non-Cryst. Solids, 351: 1967-1972.

[29] Wada S. -I., Wada K. (1982) Effects of the substitution of germanium for silicon in imogolite, Clays Clay Miner., 30: 123-128.

[30] Barron P. F., Wilson M. A., Campbell A. S., Frost R. L., (1982) Detection of imogolite in soils using solid state ^{29}Si NMR, Nature 299: 616 – 618.

[31] Ildefonse P., Kirkpatrick R. J., Montez B., Calas G., Flank A. M., Lagarde P., (1994) Investigated structure of imogolite using ^{27}Al magic-angle-spinning (MAS) NMR and aluminum X-ray absorption near edge structure, Clay. Clay Min., 42:276-287.

[32] Goodman B. A., Russell J. D., Montez B., Oldfield E., Kirkpatrick R. J., Structural studies of imogolite and allophanes by aluminum-27 and silicon-29 nuclear magnetic resonance spectroscopy, Phys. Chem. Minerals, 12:342-346.

[33] Hiradate S., Wada S. -I. (2005) Weathering process of volcanic glass to allophane determined by ^{27}Al and ^{29}Si solid-state NMR, Clay. Clay Min., 53:401-408.

[34] Hatakeyama M., Hara T., Ichikuni N., Shimazu S., (2011) Characterization of Heat-Treated Synthetic Imogolite by ^{27}Al MAS and ^{27}Al MQMAS Solid-State NMR Bull. Chem. Soc. Jpn., 84: 656–659.

[35] Henmi T., Wada K.,(1974) Surface acidity of imogolite and allopahne, Clay Minerals, 10: 231-245.

[36] Bonelli B., Ilaria Bottero I., Ballarini N., Passeri S., Cavani F., Garrone E., (2009) IR spectroscopic and catalytic characterization of the acidity of imogolite-based systems, J. Catal.,264: 15-30.

[37] Ookawa M., Onishi Y., Fukukawa S., Matsumoto K., Watanabe M., Yamaguchi T., Suzuki M. (2006) Catalytic Property of Synthetic Imogolite, Nendo Kagaku (J. Clay Sci. Soc. Japan), 45: 184-187.

[38] Ohnishi R., Tanabe K., Morikawa S., Nishizaki T. (1974) Isomerization of 2-Pinene Catalyzed by Solid Acids, Bull. Chem. Soc. Jpn. 47: 571 - 574.

[39] Ookawa M., Takata Y., Suzuki M., Inukai K., Maekawa T., Yamaguchi T. (2008) Oxidation of aromatic hydrocarbons with H_2O_2 catalyzed by a nano-scale tubular aluminosilicate, Fe-containing imogolite, Res. Chem. Inter., 34: 679-685.

[40] Mandelli D., van Vliet M. C.A, Sheldon R. A., Schuchardt U., (2001) Alumina-catalyzed alkene epoxidation with hydrogen peroxide, Appl. Cat. A, 219:209-213

[41] Monfared H. H., Amouei Z. (2004) Hydrogen peroxide oxidation of aromatic hydrocarbons by immobilized iron(III), J. Mol. Cat. A, 217: 161-164.

[42] Ookawa M., Nagamitsu Y., Oda M., Takata Y., Yamaguchi T., Maekawa T. (2008) Catalytic properties of Fe-containing imogolite in cyclohexane oxidation, Interfaces Against Pollutions 2008 Programs & Abstracts: 24.

[43] Ookawa M., Nagamitsu, Yamaguchi T., Maekawa T. (2007) Oxidation of cyclohexane Catalyzed by Fe-containing imogolite, Abstracts ISSEM2007 International Symposium on Sustainable Energy & Materials: 47.

[44] Schuchardt U., Cardoso D., Sercheli R., Pereira R., da Cruz R. S., Guerreiro M.C., Mandelli D., Spinacé E. V., Pires E. L. (2000) Cyclohexane oxidation continues to be a challenge, Appl. Cat. A 211:1-17.

[45] Ebitani K., Ide M., Mitsudome T., Mizugaki T., Kaneda K. (2002) Creation of a chain-like cationic iron species in montmorillonite as a highly active heterogeneous catalyst for alkane oxygenations using hydrogen peroxide, Chem. Comm.: 690-691.